Photon induced $\Lambda(1520)$ production and the role of the K^* exchange

Hiroshi Toki[a,b], Carmen García-Recio[a] and Juan Nieves[a]
a) Departamento de Física Atómica, Molecular y Nuclear,
Universidad de Granada, E-18071, Spain
b) Research Center for Nuclear Physics (RCNP),
Osaka University, Ibaraki, Osaka 567-0047, Japan

February 2, 2008

Abstract

We study the photon induced $\Lambda(1520)$ production in the effective Lagrangian method near threshold, $E_\gamma^{\rm LAB} \leq 2$ GeV, and in the quark-gluon string model at higher energies 3 GeV $\leq E_\gamma^{\rm LAB} \leq 5$ GeV. In particular, we study the role of the K^* exchange for the production of $\Lambda(1520)$ within the SU(6) Weinberg-Tomozowa chiral unitary model proposed in Ref. [1]. The coupling of the $\Lambda(1520)$ resonance to the $N\bar{K}^*$ pair, which is dynamically generated, turns out to be relatively small and, thus, the K exchange mechanism dominates the reaction. In the higher energy region, where experimental data are available, the quark-gluon string mechanism with the K Regge trajectory reproduces both the energy and the angular distribution dependences of the $\Lambda(1520)$ photo-production reaction.

1 Introduction

The recent announcement of the finding of the exotic hyperon, so called pentaquark, opened a new field for nuclear and particle physicists to study composite objects with more than three quarks [2, 3, 4]. A correct understanding of the experimental findings requires to possess a suitable description of hadron and photon induced reactions in a region where both, the baryon-meson and the quark-gluon degrees of freedom, should be considered, due to the energy and momentum transfers involved. On the other hand, in the recent years, our knowledge of the structure and dynamics of s-wave and d-wave odd parity baryon resonances has been increased thanks to the use of chiral unitarity schemes, which successfully generate those resonances lying near the composite hadron threshold energies [5, 6, 7, 8, 9, 10]. All these developments make this new research field exciting and worthwhile for further study.

The claimed pentaquark (Θ^+) has strangeness $S = +1$, zero isospin, a mass of around 1530 MeV and its spin–parity has not been identified yet. Definitely, all these details have to be determined and even its existence has to be investigated by further detailed experiments [11]. Due to this situation, a lot of theoretical attention is being paid to the study of the isoscalar $\Lambda(1520)$ resonance (hereafter called Λ^*), with similar mass to

that of the pentaquark, but with opposite strangeness ($S = -1$). In particular, it clearly shows up in the $K^- p$ invariant mass distribution of the two step process

$$\gamma p \to K^+ \Lambda^* \to K^+ K^- p \tag{1}$$

Note that the above reaction has a clear resemblance to the $\gamma n \to K^- \Theta^+(1530) \to K^- K^+ n$ one, where the pentaquark should appear in the $K^+ n$ mass spectrum[1]. The Λ^* spin-parity is $J^\pi = 3/2^-$, it lies slightly below the threshold energy of the $\pi\Sigma^*(1380)$ channel and it decays into a d-wave anti-kaon nucleon pair. The recent extended SU(3) chiral unitarity model of Ref. [12], which involves baryon decuplet and meson octet degrees of freedom, seems to reasonably describe the dynamics of this resonance.

There exist several effective hadron Lagrangian studies [13, 14] of the $\gamma p \to \Lambda^* K^+$ reaction for laboratory photon energies ranging from threshold, $\frac{(m_K + M_{\Lambda^*})^2 - M_N^2}{2M_N} \approx 1.7$ GeV, up to about 5 GeV, where experimental measurements are available. These theoretical studies are hampered by the lack of knowledge on the $\bar{K}^* N \Lambda^*$ coupling strength. This fact, in conjunction with the use of largely different form-factors to account for the compositeness of the hadrons, has led to contradicting predictions of the dominant reaction mechanism in the $\gamma p \to \Lambda^* K^+$ reaction. Thus, Nam et al. [13] claimed that the kaon exchange provides the leading contribution in the whole energy region, while within the quark-gluon string model of Titov et al. [14], the vector kaon (K^*) exchange turns out to be the dominant mechanism. This quark–gluon string picture was introduced by Kaidalov [15], Donnachie and Landshoff [16] more than twenty years ago, and it has been used for photon and hadron induced reactions with energies above a few GeV [17].

On the other hand, recently, a consistent SU(6) extension of the Weinberg-Tomozawa (WT) SU(3) chiral Lagrangian has been derived by García-Recio et al. [1]. In this manner, the lowest-lying meson vector nonet and baryon $3/2^+$ decuplet hadrons are considered in addition to the members of the pion and nucleon octets originally included in the WT SU(3) interaction term. The potentials deduced from this SU(6) Lagrangian are used to solve the coupled channel Bethe Salpeter Equation (BSE), within the so-called on shell Renormalization Scheme (RS), leading to unitarized s-wave meson–baryon scattering amplitudes. In what follows we will refer to this model as χSU(6)-BSE. The χSU(6)-BSE model reproduces the essential features of previous studies [5, 6, 7, 8, 9, 10] (for instance, properties of the lowest lying $J^\pi = 1/2^-$ and $3/2^-$ resonances, see for instance [18, 19]) and, in addition, it sheds some light on the role played by the vector mesons in these processes.

The model assumes that the quark interactions are spin and SU(3) flavor independent [20]. This corresponds to treating the six states of a light quark (u, d or s with spin up, $\uparrow$, or down, $\downarrow$) as equivalent. To speak meaningfully of SU(6) transformations affecting spin but not orbital angular momentum (L) as invariances, it must be assumed that the orbital angular momentum and the quark spin are to a good approximation, separately conserved. This, in turn requires the spin–orbit, tensor and spin–spin interactions between quarks to be small, which seems to be the case in the baryon spectrum. Indeed, SU(6) symmetry in the baryon sector gets some support from the large N_c limit of QCD, and it provides several predictions (relatively closeness of baryon octet and decuplet masses, the axial current coefficient ratio $F/D = 2/3$, the magnetic moment ratio $\mu_p/\mu_n = -3/2$) which are remarkably well satisfied in nature.

In the meson-baryon language, the fundamental ingredients are the mesons belonging to the $J_\pi = 0^-$ pseudoscalar octet and the $J_\pi = 1^-$ vector nonet SU(3) representations,

[1]The LEPS collaboration [2] uses a deuterium target since neutrons are unstable particles.

and the baryons of the $J^\pi = 1/2^+$ nucleon octet and of the $J^\pi = 3/2^+$ Δ decuplet. In this model, the physical masses and the physical decay constants are the only SU(6) breaking terms. After having fixed the RS, the χSU(6)-BSE model predicts, up to an overall phase, the coupling of the Λ^* resonance to the different meson-baryon channels entering in the solution of the SU(6) BSE, and in particular that to the $\bar{K}^*N$ pair. This information will help to fix the size of $t-$channel K^* exchange contribution to the Λ^* photo-production. In this respect, Hyodo and his collaborators [21] studied the $\bar{K}^*N\Lambda^*$ coupling using an effective Lagrangian to couple the K^* degrees of freedom to an extended SU(3) chiral unitarity model, which includes baryons from the decuplet. They found a rather small value, of the order of 1, for this coupling constant, while the phenomenological analysis of the photon induced reaction tends to use larger values. It is therefore important to find out this coupling in the new χSU(6)-BSE scheme, since it provides a consistent unitary chiral approach which involves also vector mesons.

The purpose of this paper is twofold. First to calculate the $\bar{K}^*N$ pair coupling to the Λ^* resonance and second to study the $\gamma p \to \Lambda^* K^+$ reaction with the new information on the role play by the K^*. For the latter one, we will use a hybrid model which combines both the hadron effective Lagrangian approach, for energies close to threshold, and the quark-gluon string reaction mechanism at higher energies.

The paper is arranged as follows. In Sect. 2, we shall discuss the effective Lagrangian model (subsection 2.1), the quark-gluon string approach (subsection 2.2) and the hybrid hadron and Reggeon exchange model (subsection 2.3) for the photon induced reaction $\gamma p \to \Lambda^* K^+$. In Sect. 3, we describe the SU(6) model. Our results are presented in Section 4. In the subsection 4.1, we extract the $\bar{K}^*$-nucleon coupling to the Λ^* resonance. In the next subsection (4.2), we discuss our results for the Λ^* photo-production from both the effective baryon-meson method and the quark-gluon string approach, and also from the hybrid model. Finally, in Sect. 5, we summarize the present study.

2 Reaction mechanisms

In this section we study the reaction

$$\gamma p \to \Lambda^* K^+ \tag{2}$$

whose total and angular differential cross sections were measured with a tagged photon beam ($2.8 < E_\gamma < 4.8$ GeV) using the LAMP2 apparatus at the 5 GeV electron synchrotron NINA at Daresbury [22].

As discussed in the introduction, we will examine two different approaches based on hadron and quark-gluon degrees of freedom, respectively, and a hybrid model based on both of them.

2.1 Effective hadron Lagrangian method

We begin with the effective Lagrangian approach, and we first list all the necessary Lagrangian densities (we are just considering charged nucleon and kaon fields, which are the only ones appearing in the tree level Feynmman diagrams; in what follows and for simplicity we will omit any explicit reference to charges when referring to coupling constants and masses),

$$\mathcal{L}_{\gamma KK} = -ie(K^- \partial^\mu K^+ - K^+ \partial^\mu K^-) A_\mu \tag{3}$$

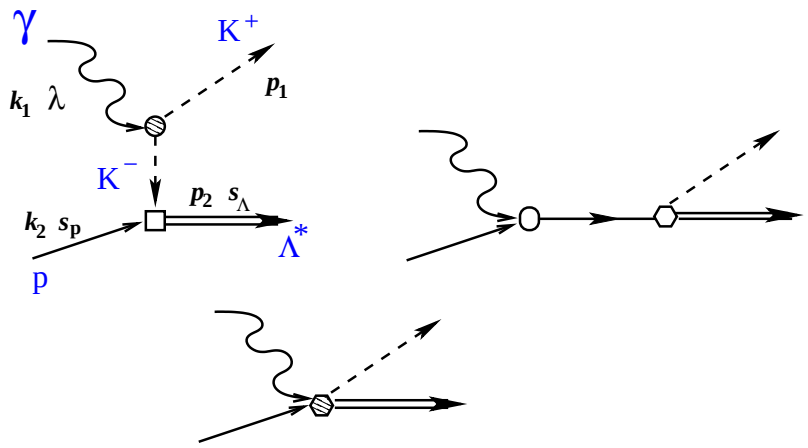

Figure 1: $\gamma p \to \Lambda^* K^+$ tree level hadron mechanisms constructed out of the Lagrangian densities given in Eqs. (3)–(6). In the first diagram we also show our definition of the kinematical (k_1, k_2, p_1, p_2) and polarization variables $(\lambda, s_\Lambda, s_p)$. In addition we use $q = k_1 - p_1$.

$$\mathcal{L}_{Kp\Lambda^*} = \frac{g_{KN\Lambda^*}}{m_K} \bar{\Lambda}^{*\mu} (\partial_\mu K^-) \gamma_5 p \ + \text{h.c.} \tag{4}$$

$$\mathcal{L}_{\gamma pp} = -e\bar{p} \left(\not{A} - \frac{\kappa_p}{2M_N} \sigma_{\mu\nu} (\partial^\nu A^\mu) \right) p + \text{h.c.} \tag{5}$$

$$\mathcal{L}_{\gamma Kp\Lambda^*} = -ie \frac{g_{KN\Lambda^*}}{m_K} \bar{\Lambda}^{*\mu} A_\mu K^- \gamma_5 p \ + \text{h.c.} \tag{6}$$

where $e = \sqrt{4\pi\alpha} > 0$, κ_p and A_μ are the proton charge, magnetic moment and photon field, respectively, and we use an obvious notation for the hadron masses, coupling constants and fields[2].

With the above Lagrangians one can construct three tree level amplitudes: i) $t-$channel kaon exchange term, ii) $s-$channel nucleon pole term and iii) contact term, which are depicted in Fig. 1. All contributions together provide a gauge invariant amplitude. We do not consider in this work the u-channel hyperon pole term which is by itself gauge invariant and related with the magnetic coupling of the photon with the Λ^*, whose information is scarce [13, 14].

Next we consider the $t-$channel K^* exchange contribution[3], we will need the Lagrangian densities,

$$\mathcal{L}_{\gamma KK^*} = e \frac{g_{\gamma KK^*}}{m_{K^*}} \epsilon^{\alpha\beta\mu\nu} (\partial_\alpha A_\beta) (\partial_\mu K^{*+}_\nu) K^- + \text{h.c.} \tag{7}$$

$$\mathcal{L}_{K^*p\Lambda^*} \ = \ \mathrm{i}\, g_{K^*N\Lambda^*} \bar{\Lambda}^*_\mu (K^{*-})^\mu p + \text{h.c.} \tag{8}$$

with $\epsilon_{0123} = +1$. The above $K^* p \Lambda^*$ vertex is predominantly $s-$wave, and its coupling constant, $g_{K^*N\Lambda^*}$ is not known. Below, we will use the χSU(6)-BSE of Ref. [1] to fix it. Thanks to the transverse nature of the $\mathcal{L}_{\gamma KK^*}$ vertex, the $t-$channel K^* exchange term is gauge invariant by itself. To compare with the works of Nam et al. [13] and Titov et

[2]We use a Rarita-Schwinger field to describe the Λ^* resonance, $K^+ = (K^-)^\dagger$ annihilates a K^+ or creates a K^- meson and p destroys a proton and $\alpha = 1/137.036$ is the fine-structure constant

[3]This contribution is readily obtained from the first diagram of Fig. 1 by replacing the exchanged kaon by a vector K^* meson.

al. [14], we have also considered a vector coupling of the $\bar{K}^* N$ pair to the Λ^* resonance, which contains a $d-$wave contribution,

$$\mathcal{L}'_{K^* p \Lambda^*} = \frac{g'_{K^* N \Lambda^*}}{m_{K^*}} \bar{\Lambda}^{*\mu} \gamma^\nu (\partial_\mu K^{*-}_\nu - \partial_\nu K^{*-}_\mu) p + \text{h.c.} \tag{9}$$

where the coupling constant $g'_{K^* N \Lambda^*}$ is not known either. We denote it with an extra prime ($g'_{K^* N \Lambda^*}$) to distinguish it from the s-wave coupling used in Eq. (8). All the other coupling constants can be fixed from the study of the K^* and Λ^* decay widths.

The contribution of the different terms of Fig. 1, including also the $t-$channel K^* exchange, to the T-matrix reads (kinematical and spin variables are explicited in the first diagram of Fig. 1)

$$-iT_i = \bar{u}_\mu(p_2, s_\Lambda) A_i^{\mu\nu} u(k_2, s_p) \epsilon_\nu(k_1, \lambda) \tag{10}$$

where u_μ and u are dimensionless Rarita-Schwinger and Dirac spinors, respectively, while $\epsilon_\nu(k_1, \lambda)$ is the photon polarization vector. The reduced $A_i^{\mu\nu}$ amplitudes related to $t-$channel K exchange are given by

$$A_t^{\mu\nu} = -e \frac{g_{KN\Lambda^*}}{m_K} \frac{1}{q^2 - m_K^2} q^\mu (q^\nu - p_1^\nu) \gamma_5 \, f_{\rm c} \tag{11}$$

$$\begin{aligned} A_s^{\mu\nu} &= -e \frac{g_{KN\Lambda^*}}{m_K} \frac{1}{s - M_N^2} \, p_1^\mu \gamma_5 \left(\not{k}_1 \, f_{\rm s} + (\not{k}_2 + M_N) \, f_{\rm c} \right) \gamma^\nu \\ &\quad -e \frac{g_{KN\Lambda^*}}{m_K} \frac{1}{s - M_N^2} \, p_1^\mu \gamma_5 (\not{k}_1 + \not{k}_2 + M_N) \mathrm{i} \, \frac{\kappa_p}{2M_N} \sigma_{\nu\rho} k_1^\rho \, f_{\rm s} \end{aligned} \tag{12}$$

$$A_c^{\mu\nu} = e \frac{g_{KN\Lambda^*}}{m_K} g^{\mu\nu} \gamma_5 \, f_{\rm c} \tag{13}$$

Here, the momentum transfer carried by the intermediate $\bar{K}$ is $q = k_1 - p_1$ and the Mandelstam variable s is defined as usual $s = (k_1 + k_2)^2$. The subindices t, s and c stand for the $t-$channel kaon exchange, the $s-$channel nucleon pole and the contact terms, respectively, and are depicted in Fig. 1. The form-factors $f_{\rm c}$ and $f_{\rm s}$ will be discussed below. We define

$$T_K = T_t + T_s + T_c, \tag{14}$$

and in what follows we will refer to it as the K mechanism contribution to the $T-$matrix. Similarly, for the K^* contribution we get

$$A_v^{\mu\nu} = -e \frac{g_{\gamma K K^*}}{m_{K^*}} \frac{g_{K^* N \Lambda^*}}{q^2 - m_{K^*}^2} \epsilon^{\alpha\nu\beta\mu} k_{1\alpha} q_\beta \, f_{\rm v} \tag{15}$$

For comparison with previous studies, we also write this contribution for the case of the vector coupling of Eq. (9)

$$A_{v'}^{\mu\nu} = -e \frac{g_{\gamma K K^*}}{m_{K^*}} \frac{g'_{K^* N \Lambda^*}}{q^2 - m_{K^*}^2} k_{1\alpha} q_\beta \left(\epsilon^{\alpha\nu\beta\mu} \frac{\not{q}}{m_{K^*}} - \frac{q^\mu}{m_{K^*}} \epsilon^{\alpha\nu\beta\sigma} \gamma_\sigma \right) f_{\rm v} \tag{16}$$

where here again the form-factor $f_{\rm v}$ will be discussed below. We remind here that $\not{q} = M_{\Lambda^*} - M_N$, and $-q^\mu u_\mu(p_2, s_\Lambda) = k_2^\mu u_\mu(p_2, s_\Lambda)$ for on-shell baryons. The first term in Eq. (16) is of the type of the contribution in Eq. (15), and it is plausible to expect similar values for $g'_{K^* N \Lambda^*}$ and $g_{K^* N \Lambda^*}$, since $(M_{\Lambda^*} - M_N)/M_{K^*} \approx 2/3$. The second term in Eq. (16) is generated by a $K^{*-} p$ d-wave coupling to the Λ^* resonance. In general the interaction of Eq. (9) contains two independent components. In terms of multipoles, they

are $E1$ and $M2$. In the $E1$ amplitude, the orbital angular momentum of the decaying channel $K^{*-}p$ is s-wave, while in $M2$, it is d-wave. The $E1$ ($M2$) amplitude is dominated by the first (second) term in Eq. (16). We expect that the s-wave coupling will dominate near Λ^* threshold, where all involved three momenta at the hadron vertex are small. We will apply the effective Lagrangian method only near the threshold energy, $\sqrt{s} \approx 2$ GeV, and thus we do not expect sizable effects arising from the second term in Eq. (16). In the recent work of Hyodo et al., [21], it is also argumented the dominance of the s-wave $K^*N\Lambda^*$ component of vertex at low and intermediate energies.

The K^* mechanism contribution to the $T-$matrix is given by one of the above expressions, $T_{K^*} = T_v$ or $T_{K^*} = T_{v'}$.

Up to this point, the T-matrix is gauge invariant. However, we ought to introduce the compositeness of the hadrons. This is usually achieved by including form-factors in the amplitudes in such manner that gauge invariance is preserved[4]. There is no unique theoretical way to introduce the form-factors, this was discussed at length by Ohta [24] and by Haberzettl et al. [25]. We adopt here the scheme used in the previous works [13, 14], where the prescription of Ref. [25] was used. We take the following parameterization for the form-factors

$$f_{\rm i} = \frac{\Lambda^4}{\Lambda^4 + (q_{\rm i}^2 - M_{\rm i}^2)^2}, \quad {\rm i} = {\rm s, t, v} \tag{17}$$

$$f_{\rm c} = f_{\rm s} + f_{\rm t} - f_{\rm s} f_{\rm t}, \quad \text{and} \quad \left\{ \begin{array}{l} q_{\rm s}^2 = s,\, q_{\rm t}^2 = q_{\rm v}^2 = q^2 \\ M_{\rm s} = M_N,\, M_{\rm t} = m_K,\, M_{\rm v} = m_{K^*} \end{array} \right. \tag{18}$$

In the expressions of the different contributions to T_K and T_{K^*}, given in Eqs. (11)-(13) and Eqs. (15)-(16), we have already included the form-factors. The form of $f_{\rm c}$ is chosen such that the on-shell values of the coupling constants are reproduced.

2.2 String quark-gluon reaction mechanism

We introduce now the quark-gluon reaction mechanism, based on the work of Kaidalov [15, 26]. It is obvious from the analysis of the experimental hadron cross section data that the Reggeon and the Pomeron exchange mechanisms play a crucial role at high energies, which was nicely demonstrated by Donnachie and Landshoff [16]. Kaidalov demonstrated that the quark-gluon mechanism involves the formation of the QCD string between colored objects formed by high energy collisions and the reaction cross section could be related with the Regge-slope, α', and the intercept, $\alpha(0)$, in the Reggeon exchange model. Hence the reaction $\gamma p \to K^+\Lambda^*$ can be described by the exchange of two valence (u and $\bar{s}$) quarks in the $t-$channel with any number of gluon exchanges between them. Alternatively, in terms of the Regge phenomenology, it corresponds to a Reggeon (R) exchange, and thus the scattering amplitude reads,

$$T_{qgR} = \frac{\bar{g}_{\gamma KR}\bar{g}_{RN\Lambda^*}}{M_R}(-s/s_0)^{\alpha(t)}F(t) \tag{19}$$

following the work of Grishina et al. [17]. $F(t)$ is a form-factor which accounts for the compositeness of the external (incoming and outgoing) hadrons with $t = q^2$, the squared of the four momentum transfer. We take $F(t) = F_{\gamma K}(t)F_{p\Lambda^*}(t)$ with gaussian forms for

[4]For the sake of brevity and to avoid repeating similar equations, in Eqs. (11)-(13) and Eqs. (15)-(16), we have already included form-factors. Details are given in what follows.

each of the vertices, i.e. $F_\beta(t) = \exp(t/a_\beta^2)$, and then the combined one is also of gaussian type,

$$F(t) = \exp(t/a^2) \tag{20}$$

The constant s_0 is taken as the Mandelstam variable s at threshold ($s_0 = (m_K + M_{\Lambda^*})^2$), and it is introduced to fix the dimensions and to normalize the coupling constants. On the other hand, $\alpha(t) = \alpha(0) + \alpha' t$ is the Regge trajectory associated to the Reggeon quantum numbers. We can choose any of the $K-$ or K^*-trajectories or considering both; we denote the different possibilities by R in Eq. (19). On the other hand, it is customary to fix the coupling constants to those used in the effective hadron Lagrangian approach. However, this is not necessarily true, since the exchanged Reggeon has its own extended quark-gluon structure, and it does not have to couple to the external hadrons with the same strength as the virtual exchanged meson does within the effective Lagrangian model. In addition, the strength of the couplings will also depend on the election of s_0. In Eq. (19), we use bars ($\bar{g}'s$) to differentiate the couplings constants from those appearing in the previous subsection. The parameter a in Eq. (20), which controls the $t-$exponential decrease of the form factor and the coupling constants will be fixed to the experimental data.

The spin structure of the Reggeon exchange comes from the quark rearrangement process [27], for simplicity we do not consider it in this study and thus, we consider the Regge amplitude independent of the incoming and outgoing particle helicities.

2.3 Hybrid hadron and Reggeon exchange model

We propose a hybrid mechanism to study the $\gamma p \to \Lambda^* K^+$ reaction in a wide range of laboratory photon energies. At low energies, near threshold, we consider the effective Lagrangian model discussed in Subsect. 2.1, while for higher photon energies we assume that the string quark-gluon mechanism is dominant. We will implement a smooth transition between both reaction mechanisms for laboratory photon energies around 2.5 GeV. The invariant differential cross section, $d\sigma/dt$ reads

$$\frac{d\sigma}{dt} = \frac{1}{4\pi} \frac{M_N M_{\Lambda^*}}{(s - M_N^2)^2} \left(\frac{1}{4} \sum_{\lambda, s_p, s_\Lambda} |T|^2 \right) \tag{21}$$

where the invariant Mandelstam variable $t = (k_1 - p_1)^2$ varies in the range $t_- \leq t \leq t_+$, with $t_\pm = m_K^2 - 2|\vec{k}_1^{\,\rm cm}| \left(p_1^0 \mp |\vec{p}_1| \right)^{\rm cm}$, with variables defined, for instance, in the center of mass (cm) frame. It is also of interest the angular differential cross section in the cm frame, which is related to $d\sigma/dt$ by

$$\left. \frac{d\sigma}{d\Omega} \right|_{\rm cm} = \frac{|\vec{k}_1^{\,\rm cm}||\vec{p}_1^{\,\rm cm}|}{\pi} \frac{d\sigma}{dt} \tag{22}$$

The sum over polarizations is trivially done for the Regge amplitude, since we have neglected any spin dependence in that case. In the case of the effective Lagrangian approach, it can be easily done thanks to

$$\sum_\lambda \epsilon^\mu(k_1, \lambda) \epsilon^{\nu *}(k_1, \lambda) = -g^{\mu\nu} + \cdots \tag{23}$$

where the terms $\cdots$ are proportional to k_1^μ and/or k_1^ν and do not contribute because of gauge invariance, and the traditional expressions for the sum of Dirac and Rarita-

Schwinger spinors. In this latter case, we use

$$\begin{aligned}\sum_{s_\Lambda} u^\mu(p_2,s_\Lambda)\bar{u}^\nu(p_2,s_\Lambda) &= -\frac{\not{p}_2+M_{\Lambda^*}}{2M_{\Lambda^*}}P^{\mu\nu}(p_2)\\ P^{\mu\nu}(p_2) &= \left(g^{\mu\nu}-\frac{1}{3}\gamma^\mu\gamma^\nu-\frac{2}{3}\frac{p_2^\mu p_2^\nu}{M_{\Lambda^*}^2}+\frac{1}{3}\frac{p_2^\mu\gamma^\nu-p_2^\nu\gamma^\mu}{M_{\Lambda^*}}\right)\end{aligned} \tag{24}$$

Finally, we get

$$\frac{1}{4}\sum_{\lambda,s_p,s_\Lambda}|T|^2 = \frac{1}{16M_NM_{\Lambda^*}}g_{\nu\sigma}\mathrm{Tr}\left((\not{p}_2+M_{\Lambda^*})P_{\rho\mu}(p_2)A^{\mu\nu}(\not{k}_2+M_N)\gamma^0(A^{\rho\sigma})^\dagger\gamma^0\right) \tag{25}$$

with

$$A^{\mu\nu}=\sum_i A_i^{\mu\nu}, \qquad i=s,c,t,v \text{ or } v' \tag{26}$$

We construct the $T-$matrix as a weighted combination of the two reaction mechanism contributions,

$$\begin{aligned}T &= T(\text{hadron})\left(1-g(E_\gamma^{\text{LAB}})\right)+T(\text{quark})g(E_\gamma^{\text{LAB}}),\\ &\quad T(\text{hadron})=T_K+T_{K^*}, \qquad T(\text{quark})=T_{qgR}.\end{aligned} \tag{27}$$

and for the weighting function $g(E)$, we use

$$g(E)=\frac{1}{1+exp(-(E-E_0)/\Delta E)} \tag{28}$$

We will fix E_0 and ΔE by comparing with the experimental data.

3 SU(6) WT unitary model (χSU(6)-BSE) and the $\Lambda(1520)$ resonance

The WT interaction Lagrangian, which is the leading contribution in the chiral counting, has been the starting point of all SU(3) chiral unitarity approaches developed in the recent years to study meson-baryon s-wave scattering. As discussed in the introduction, SU(6) spin-flavor symmetry might provide a reasonable framework where to incorporate baryon decuplet and vector meson nonet degrees of freedom in the study of hadron processes at low energies. A consistent SU(6) extension of the WT SU(3) chiral Lagrangian was presented in Ref. [1], and its generalization to an arbitrary number of colors and of colors and flavors can be found in Refs. [28] and [29], respectively.

Following Ref. [1], the building blocks of this extension are the {35} and {56} representations[5] of SU(6). The first one is the adjoint representation of the SU(6) group, and its SU(3) multiplet and SU(2) spin content is

$$\{35\}=8_1+8_3+1_3 \tag{29}$$

where we denote a SU(3) multiplet μ of spin J by μ_{2J+1}. Hence, the pseudoscalar meson octet (K, π, η and $\bar{K}$), and the vector meson nonet (K^*, ρ, ω, $\bar{K}^*$ and ϕ) belong to the same SU(6) representation,{35}. The lowest mass baryons belong to the {56}

[5]We label the SU(6) multiplets by a number, which is their dimensionality, enclosed between curly brackets.

representation of SU(6), which is totally symmetric allowing the baryon to be made of three quarks in $s-$wave. Its spin-flavor (isospin and hypercharge) content is determined by the decomposition

$$\{56\} = 8_2 + 10_4 \tag{30}$$

and it accommodates the spin $1/2^+$ members of the nucleon octet (N, Σ, Λ and Ξ) and the spin $3/2^+$ members of the Δ decuplet (Δ, Σ^*, Ξ^* and Ω).

We denote a meson state as $\mathcal{M} = [(\mu_M)_{2J_M+1}, I_M, Y_M]$, where J_M, I_M, Y_M are the spin, isospin and the hypercharge quantum numbers of the meson. We use a similar notation for baryon states $\mathcal{B}$. The meson-baryon states are then expressed in terms of the SU(6) coupled basis, $\left|\phi; \mu^{\alpha}_{2J+1} IY\right\rangle$, as

$$\begin{aligned} |\mathcal{MB}; JIY\rangle = & \sum_{\mu,\alpha,\phi} \left(\begin{array}{cc|c} \mu_M & \mu_B & \mu \\ I_M Y_M & I_B Y_B & IY \end{array} \right) \\ & \times \left(\begin{array}{cc|c} 35 & 56 & \phi \\ \mu_M J_M & \mu_B J_B & \mu J\alpha \end{array} \right) \left|\phi; \mu^{\alpha}_{2J+1} IY\right\rangle \, , \end{aligned} \tag{31}$$

where the first and second factors in the linear combination are SU(3) and SU(6) Clebsh-Gordan coefficients, respectively, and are given in Refs. [30] and [31]. In the SU(6) coupled basis, ϕ stands for the SU(6) irreducible representations ($\phi = \{56\}$, $\{70\}$, $\{700\}$ and $\{1134\}$, from the reduction into irreducible representations of the product $\{35\} \otimes \{56\}$) and α accounts for possible multiplicity of each of the μ_{2J+1} SU(3) multiplets of spin J.

The assumption that the s-wave meson-baryon potential, V, is a SU(6) invariant operator implies that $|\phi; \mu^{\alpha}_{2J+1} IY\rangle$ coupled states are eigenvectors of the potential and the corresponding eigenvalues ($V_\phi(s)$), besides the Mandelstam variable s, depend only on the SU(6) representation ϕ, being thus independent of the other quantum numbers, μ, α, J, I, Y. Hence, the matrix elements of the potential can be written as

$$V^{JIY}_{\mathcal{MB},\mathcal{M}'\mathcal{B}'}(s) = \langle \mathcal{M}', \mathcal{B}'; JIY | V | \mathcal{M}, \mathcal{B}; JIY \rangle = \sum_{\phi} V_\phi(s) \mathcal{P}^{\phi,JIY}_{\mathcal{MB},\mathcal{M}'\mathcal{B}'} \tag{32}$$

with the projection operators given by

$$\begin{aligned} \mathcal{P}^{\phi,JIY}_{\mathcal{MB},\mathcal{M}'\mathcal{B}'} = & \sum_{\mu,\alpha} \left(\begin{array}{cc|c} 35 & 56 & \phi \\ \mu_M J_M & \mu_B J_B & \mu J\alpha \end{array} \right) \\ \times & \left(\begin{array}{cc|c} \mu_M & \mu_B & \mu \\ I_M Y_M & I_B Y_B & IY \end{array} \right) \left(\begin{array}{cc|c} \mu'_{M'} & \mu'_{B'} & \mu \\ I'_{M'} Y'_{M'} & I'_{B'} Y'_{B'} & IY \end{array} \right) \\ \times & \left(\begin{array}{cc|c} 35 & 56 & \phi \\ \mu'_{M'} J'_{M'} & \mu'_{B'} J'_{B'} & \mu J\alpha \end{array} \right) . \end{aligned} \tag{33}$$

We are now in a position to extract the four SU(6) eigenvalues by relating them to those of the SU(3) matrix elements of the WT interaction. The mesons of the pion octet and the baryons of the nucleon octet interact through the WT Lagrangian, being the corresponding potential [5, 6, 7, 9]

$$V^{IY}_{ij}(\sqrt{s}) \;\; = \;\; D^{IY}_{ij} \frac{\sqrt{s} - M}{2\, f^2} \tag{34}$$

where the indices i and j identify the final and initial meson-baryon pair (quantum

numbers $I'_{M'}Y'_{M'}I'_{B'}Y'_{B'}$ and $I_MY_MI_BY_B$, respectively) and

$$\begin{aligned} D_{ij}^{IY} &= \sum_{\mu,\gamma,\gamma'} \lambda_{\mu_\gamma \to \mu_{\gamma'}} \left(\begin{array}{cc|c} 8 & 8 & \mu_\gamma \\ I_MY_M & I_BY_B & IY \end{array} \right) \\ &\times \left(\begin{array}{cc|c} 8 & 8 & \mu_{\gamma'} \\ I'_{M'}Y'_{M'} & I'_{B'}Y'_{B'} & IY \end{array} \right) \end{aligned} \tag{35}$$

Here, M is the baryon mass, $f \simeq 93\,\mathrm{MeV}$ the pion weak decay constant, μ runs over the 27, 10, 10^*, 8 and 1 SU(3) representations and γ, γ' are used to account for the two octets (8_s and 8_a) that appear in the reduction of $8 \otimes 8$. The SU(3) eigenvalues λ's, are $\lambda_{27} = 2$, $\lambda_{8_s} = \lambda_{8_a} = -3$, $\lambda_1 = -6$, $\lambda_{10} = \lambda_{10^*} = \lambda_{8_s \leftrightarrow 8_a} = 0$ [10]. Note how chiral symmetry determines all eigenvalues, which otherwise will be totally independent and unknown for a generic SU(3) symmetric theory.

To deduce the SU(6) eigenvalues, we study the reduction of the SU(6) matrix elements of Eqs. (32)-(33) when only the pion and nucleon octets are considered. It is clear that not all SU(3) invariant interactions in the (8_1)meson–(8_2)baryon sector can be extended to a SU(6) invariant interaction. Remarkably, the seven couplings (λ's) in the WT interaction turn out to be consistent with SU(6) and moreover, the extension is unique. Indeed, we find that by taking

$$V_\phi(s) = \bar{\lambda}_\phi \frac{\sqrt{s} - M}{2\,f^2}\,, \tag{36}$$

with the coefficients $\bar{\lambda}$'s given by

$$\bar{\lambda}_{56} = -12, \quad \bar{\lambda}_{70} = -18, \quad \bar{\lambda}_{700} = 6, \quad \bar{\lambda}_{1134} = -2, \tag{37}$$

the SU(3) matrix elements described above (Eqs. (34)-(35)) are completely reproduced. As it is discussed in Ref. [1], the underlying chiral symmetry of the WT Lagrangian has made possible the spin symmetry extension presented here.

Next we consider explicit SU(6) breaking effects due to the use of physical (experimental) hadron masses and meson decay constants. Hence in Eq. (36), we make the replacement

$$\frac{\sqrt{s} - M}{2f^2} \to \frac{2\sqrt{s} - M_i - M_j}{4 f_i f_j} \tag{38}$$

To describe the dynamics of resonances one needs to have exact elastic unitarity in coupled channels. For that purpose, we solve the coupled channel BSE and use the SU(6) potential defined above to construct its interaction kernel. In a given JIY sector, the solution for the coupled channel $s-$wave scattering amplitude, T^J_{IY}, satisfies exact unitarity in coupled channels. In the so called *on-shell* scheme [10], and normalized as the t matrix defined in Eq. (33) of the first entry of Ref [9], it is given by

$$T^J_{IY}(s) = \frac{1}{1 - V^J_{IY}(s) J^J_{IY}(s)} V^J_{IY}(s) \tag{39}$$

where $J^J_{IY}(s)$ is a diagonal function in the coupled channel space. Suppressing the indices, it is written for each channel as

$$J(s) = \frac{(\sqrt{s} + M)^2 - m^2}{2\sqrt{s}} J_0(s) \tag{40}$$

$$J_0(s) = i \int \frac{d^4k}{(2\pi)^4} \frac{1}{(P-k)^2 - M^2 + i\epsilon} \frac{1}{k^2 - m^2 + i\epsilon} \tag{41}$$

where M and m are the masses of the baryon and meson corresponding to the channel and P^μ is the total meson-baryon four momentum ($P^2 = s$). On the other hand, $J_0(s)$ involves a logarithmic divergence which needs to be subtracted,

$$J_0(s) = \bar{J}_0(s) + J_0(s = (M+m)^2) \tag{42}$$

where the finite $\bar{J}_0(s)$ function can be found in Eq. (A9) of the first entry of Ref [9]). It induces the unitarity right hand cut of the amplitude. Besides, the constant $J_0(s = (M+m)^2)$ hides the logarithmic divergence. It is renormalized by requiring

$$J_0(s = \mu_0^2) = 0 \tag{43}$$

at a certain scale μ_0. This defines our RS. A suitable choice is to take μ_0 independent of J and set it uniformly within a given IY sector as $\sqrt{m_{\rm th}^2 + M_{\rm th}^2}$, where $(m_{\rm th} + M_{\rm th})^2$ gives the smallest threshold among all channels involved in a IY sector [8].

Particularly for the $\Lambda(1520)$ state, with quantum numbers $I = 0$, $Y = 0$ and $J^\pi = 3/2^-$, we have a total of 9 channels in the SU(6) scheme: $\pi\Sigma^*$, $\bar{K}^*N$, $\omega\Lambda$, $\rho\Sigma$, $K\Xi^*$, $\phi\Lambda$, $\rho\Sigma^*$, $K^*\Xi$ and $K^*\Xi^*$. The potential thus reads,

$$V^{(3/2,0,0)} = D^{(3/2,0,0)} \frac{2\sqrt{s} - M_i - M_j}{4 f_i f_j} \tag{44}$$

where the symmetric coupled channel matrix $D^{(3/2,0,0)}$ is obtained from Eqs. (32)-(33) and (36)-(37). It is given by

$$D^{(3/2,0,0)} = \tag{45}$$

$$\begin{pmatrix}
-4 & -\sqrt{2} & 0 & -4/\sqrt{3} & -\sqrt{6} & 0 & -\sqrt{80/3} & \sqrt{2} & -\sqrt{10} \\
 & 0 & \sqrt{6} & \sqrt{2/3} & 0 & 0 & \sqrt{10/3} & 0 & 0 \\
 & & 0 & 2 & \sqrt{2} & 0 & \sqrt{20} & -\sqrt{2/3} & \sqrt{10/3} \\
 & & & -8/3 & -\sqrt{2} & 0 & -\sqrt{20/9} & \sqrt{2/3} & -\sqrt{10/3} \\
 & & & & -3 & -2 & -\sqrt{10} & 0 & -\sqrt{15} \\
 & & & & & 2 & 0 & \sqrt{16/3} & \sqrt{20/3} \\
 & & & & & & -16/3 & \sqrt{10/3} & -\sqrt{50/3} \\
 & & & & & & & -4/3 & \sqrt{80/9} \\
 & & & & & & & & -11/3
\end{pmatrix}
\begin{matrix}
\pi\Sigma^* \\ \bar{K}^*N \\ \omega\Lambda \\ \rho\Sigma \\ K\Xi^* \\ \phi\Lambda \\ \rho\Sigma^* \\ K^*\Xi \\ K^*\Xi^*
\end{matrix}$$

Note we assume an ideal mixing in the vector meson sector, i.e., $\omega = \frac{1}{\sqrt{2}}\left(u\bar{u} + d\bar{d}\right)$ and $\phi = s\bar{s}$, which induces the use of some linear combinations of the isoscalar SU(3) vector meson mathematical states[6].

We include an explicit breaking of the SU(6) symmetry through the use of the experimental masses and the meson decay constants: $f_\pi = 92.4$ MeV [23], $f_K = 113.0$ MeV [23], $f_\rho = f_{K^*} = 153$ MeV (from $\Gamma(\rho \to e^+e^-)$, $\Gamma(\tau \to \rho\nu_\tau)$, and $\Gamma(\tau \to K^*\nu_\tau)$), $f_\phi = 163$ MeV (from $\Gamma(\phi \to e^+e^-)$) and $f_\omega \approx f_\rho$.

[6]In the vector meson sector, Carter's SU(6)–multiplet coupling factors [31] are consistent with the election of $\phi_1 = \frac{1}{\sqrt{3}}\left(u\bar{u} + d\bar{d} + s\bar{s}\right)$ and $\phi_8 = -\frac{1}{\sqrt{6}}\left(u\bar{u} + d\bar{d} - 2s\bar{s}\right)$ quark wave functions for the SU(3) singlet and isospin singlet of the SU(3) octet, respectively. The relative minus sign is absent in the pseudoscalar meson sector.

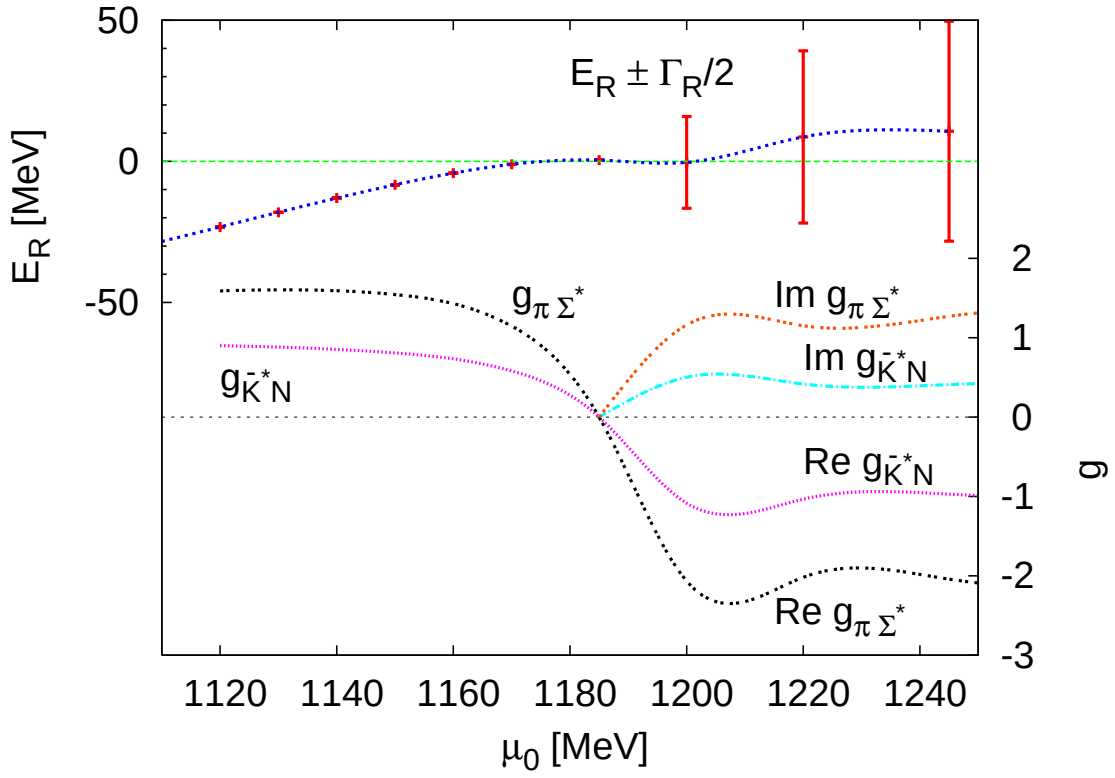

Figure 2: χSU(6)-BSE predictions for the Λ^* resonance pole position ($M_R = m_\pi + M_{\Sigma^*} + E_R$, Γ_R) and couplings (Eq. (48)) to the $\pi\Sigma^*$ and $\bar{K}^*N$ channels as function of the renormalization scale μ_0.

4 Results and discussion

We use $M_{\Lambda^*} = 1519.5$ MeV and charged nucleon, kaon and K^* masses from the PDG [23]. Besides, we use $eg_{\gamma KK^*} = 0.23$ and $g_{KN\Lambda^*} = 10.5$ from the $K^{*+} \to K^+\gamma$ radiative[7], and the Λ^* decay widths[8], respectively. Thus the only unknown parameters in the effective Lagrangian approach are $g_{K^*N\Lambda^*}$ and the cutoff Λ entering in the hadron form-factors of Eq. (18).

4.1 The coupling $g_{K^*N\Lambda^*}$

We study here the dynamics of Λ^* resonance within the SU(6) model presented in Sect. 3 Without including the vector mesons in the model, there exist only two channels which

[7]From the Lagrangian of Eq. (7), we obtain

$$\Gamma = \frac{1}{96\pi}\left(eg_{\gamma KK^*}\right)^2 m_{K^*}\left(1-\frac{m_K^2}{m_{K^*}^2}\right)^3 \approx 50.3 \text{ KeV [23]} \tag{46}$$

[8]From the Lagrangian of Eq. (4), we obtain for the $\Lambda^* \to pK^-$ decay width

$$\Gamma = \frac{1}{12\pi}\frac{g_{KN\Lambda^*}^2}{m_K^2}|\vec{p}_{cm}|^3\frac{M_{\Lambda^*}-p_{cm}^0-M_N}{M_{\Lambda^*}} \approx \frac{1}{2}0.45\times 15.6 \text{ MeV [23]}. \tag{47}$$

where p_{cm}^μ is the antikaon four momentum in the Λ^* rest frame.

contribute to the formation of the Λ^* state, which are π-Σ^* and K-Ξ^*. Since the mass of Λ^* resonance is very close to the threshold energy of the π-Σ^* channel ($\approx 1520 - 1525$ MeV), this channel dominates the dynamics of Λ^*. When the vector meson degrees of freedom are taken into account, there are appear seven additional channels. However, the dynamics of the Λ^* resonance is almost unaffected by the heavier ones. Thus in very good approximation, we have considered the 4×4 sub-matrix of $D^{(3/2,0,0)}$ constructed out the first four rows and columns (π-Σ^*, $\bar{K}^*$-N, ω-Λ and ρ-Σ). We solve the coupled channel BSE and renormalize the amplitudes as described above in Eqs. (39)–(43). We look for complex poles of the $T-$matrix in the Second Riemann Sheet (SRS), determined by continuity to the First Riemann Sheet (FRS) [9]. In a given JIY sector, physical resonances appear in the SRS of all matrix elements of $T(s)$ (Eq. (39)), in the coupled channel space, differing only on the value of the residue at the pole. The pole position determines the mass and width of the resonance, while the different residues for each meson-baryon channel give the respective couplings and branching ratios (see section II.D of the second entry of Ref. [9]). Let us consider $s_R = M_R^2 - \mathrm{i}\, M_R \Gamma_R$ a pole in the SRS of the coupled channel scattering matrix $T(s)$. Then, around the pole, it can be approximated by

$$[T(s)]_{ij} \;\approx\; 2M_R \frac{g_i g_j}{s - s_R}, \tag{48}$$

where $g_i g_j$ is the residue matrix. The complex vector g_i determines the coupling of the resonance to the different final states, which are well and unambiguously defined even if the corresponding channels are closed in the decay of the resonance.

As discussed above, after Eq. (43), to describe the $I = 0, Y = 0$ sector, our standard choice would be $\mu_0 = \sqrt{m_\pi^2 + M_\Sigma^2} \approx 1.2$ GeV, for which we find a pole with $M_R = 1528$ MeV and $\Gamma_R = 42$ MeV. This is a remarkable result, since the SU(6) model predicts the existence of the Λ^* resonance. Within the model, it appears slightly above the $\pi\Sigma^*$ threshold and that originates a non-vanishing width, since the $\pi\Sigma^*$ channel is open. Experimentally, the mass of the resonance is 1519.5 MeV, around 3 MeV below the $\pi\Sigma^*$ threshold, and its width is around 15.6 MeV (it decays predominantly into d-wave $\pi\Sigma$ and $\bar{K}N$ pairs and the three body mode $\Lambda\pi\pi$, none of them considered in the SU(6) model). To better describe the dynamics of the resonance, we have varied the renormalization scale in the vicinity of 1.2 GeV. Results are displayed in Fig. 2. For values of μ_0 below 1185 MeV, the pole appears in the FRS and therefore it should be interpreted as $\pi\Sigma^*$ bound state. Within our model it would be stable (zero width), since none of the allowed decay modes ($\pi\Sigma$, $\bar{K}N$ and $\Lambda\pi\pi$) are included in our two body s-wave approach. Scales in the range 1160-1185 MeV provide masses around 1520 MeV. In the figure we also show the couplings (Eq. (48)) of the resonance Λ^* to the $\pi\Sigma^*$ and $\bar{K}^*N$ channels ($g_{\pi\Sigma^*}$ and $g_{\bar{K}^*N}$, respectively). We would like to make three remarks.

- Both couplings are determined up to an overall minus sign.
- The coupling $g_{K^*N\Lambda^*}$ (defined in Eq. (8)) is given by $g_{\bar{K}^*N}/\sqrt{2}$, where the $\sqrt{2}$ factor comes trivially from the projection of the pK^{*-} state into isospin zero.
- Both couplings vanish when the Λ^* resonance is placed just at the $\pi\Sigma^*$ threshold. It is to say, when the resonance can be interpreted as $\pi\Sigma^*$ state bound with zero energy.

The latter remark has important phenomenological repercussions, since the actual position of the Λ^* is quite close to the $\pi\Sigma^*$ threshold and it would imply that $g_{K^*N\Lambda^*}$ coupling should be much smaller (we read off from the figure a value around $0.75/\sqrt{2}$) than the

values used in the phenomenological analysis of Refs. [13, 14]. It is easy to understand this behavior of the coupling constants. Let us start studying the simple case of the elastic scattering of a meson of mass m off a baryon of mass M. The s-wave scattering amplitude close to threshold can be then approximated by

$$f(p) = \frac{e^{2\,\mathrm{i}\delta(p)} - 1}{2\,\mathrm{i}p} \approx \frac{1}{-\frac{1}{\alpha} + \frac{1}{2}r_0^2 p^2 + ... - ip}, \quad p^2 = 2\mu E,\ s \approx s_{\rm th} + 2(m+M)E \tag{49}$$

with α and r_0 the scattering length and effective range, respectively. Besides, $s_{\rm th} = (m+M)^2$ and μ is the reduced mass. If there exist a bound state at $s = s_B$ very close to threshold[9], one can drop the scattering range term and the scattering length can be approximated by $\alpha \sim \frac{1}{\sqrt{2\mu|E_B|}}$, where $E_B(<0) = (s_B - s_{\rm th})/2\sqrt{s_{\rm th}}$ is the binding energy of the bound state. In this situation for both above ($E > 0$) and below ($E < 0$) threshold, but close to it, f can be written as

$$f(p) \approx \frac{-1}{\sqrt{2\mu}} \frac{\sqrt{-E} + \sqrt{-E_B}}{E - E_B}, \tag{50}$$

and therefore the residue of the f at the pole is given by $-\sqrt{2|E_B|/\mu}$. Since the scattering amplitude and the T-matrix close to threshold are related by $f \approx -\frac{M}{4\pi(m+M)}T$, from Eq. (48) we obtain

$$g^2 = 4\pi \frac{m}{\mu} \sqrt{\frac{2|E_B|}{\mu}} \tag{51}$$

Therefore the square of the coupling of the bound state to the channel scales like the square root of the binding energy. The same result can be found just by looking directly for poles of T (Eq. (39)) in the FRS. Indeed, following Ref. [10], the position of the pole, s_B, is such that the dimensionless function

$$\beta(s) = \frac{2f^2}{J(s)(\sqrt{s} - M)}, \tag{52}$$

at $s = s_B$, becomes[10] D. In addition,

$$g^2 = D^2 \frac{\sqrt{s_B} - M}{2f^2} \frac{1}{\beta'(s_B)} \tag{53}$$

and it reduces to Eq. (51) when s_B is close to threshold. The behaviour of g^2 with $|E_B|$ follows from the behaviour of $dJ/ds|_{s_B}$ when s_B is close to $s_{\rm th}$, where it diverges like $1/\sqrt{s_{\rm th} - s_B} \approx (2(m+M))^{-1/2}/\sqrt{|E_B|}$, and therefore $\beta'(s_B)$ does also diverge in that limit.

Similar conclusions can be drawn in the general case, when coupled channels are considered. However, in that case, D, β and J are matrices and some subtleties appear. Nevertheless, the behavior of the coupling of the bound state to the different channels can be analytically worked out. We find that, if there exists a bound state very close to the smallest of the thresholds (let us take an ordering such that this channel is the first one), the sum of the squares of the couplings of this bound state to the different channels

[9] It is to say, the scattering amplitude has a pole for a real value of $s = s_B \leq s_{\rm th}$. In Fig. 2, it would correspond to $E_R \leq 0$.

[10] In the case of only one channel, D is a 1×1 matrix, it is to say a real number.

vanishes as the binding energy approaches to zero. Indeed, it can be proved that this sum scales again as $\sqrt{|E_B|}$, i.e.

$$\sum_i g_i^2 = \frac{1}{c^2 \frac{1}{4\pi \frac{m}{\mu}\sqrt{\frac{2|E_B|}{\mu}}} + \cdots} \tag{54}$$

where c is a coefficient related with the projection of the resonance wave function into the first channel, m and M are the masses of the meson and baryon in this channel, $E_B = (s_B - (m+M)^2)/2(m+M)$, and the dots stand for some contributions which remain finite in the $|E_B| \to 0$ limit. Note that the sum over i in the above equation runs over all channels, and since all couplings are real, it implies that all terms in the sum must vanish. For $|E_B| \approx 2.5$ MeV, we find $\sum_i g_i^2 \approx 2.75$, which is largely saturated by $g_{\pi\Sigma^*}$, leaving little room for $g_{\bar{K}^*N}$.

Of course, if one is working with an unique channel, $c = 1$, we recover Eq. (51). However, if the resonance does not couple to the first channel, $c = 0$ and $g_1 = 0$, then we cannot conclude anything about the rest of the couplings.

The results of Fig. 2 favor values of the coupling constant $g_{K^*N\Lambda^*}$ around 0.5 or smaller, which, following the discussion below Eq. (16), will correspond to a value of $g'_{K^*N\Lambda^*}$ of about 0.75 and it constitutes one of the major results of this work. This value is significantly smaller than the values of around 10 used in the phenomenological analysis of Nam et al. [13] and Titov et al. [14]. From the discussion above and taking into account the proximity of the Λ^* to the $\pi\Sigma^*$ threshold, we have compelling reasons to expect such a small value for this coupling constant.

Hyodo et al. [21] find $g'_{K^*N\Lambda^*} \sim 1.5/\sqrt{2}$ within an extended SU(3) chiral unitary model[11], which accounts for the baryons of the decuplet and for some d-wave contributions, and where an effective Lagrangian is used to include the $\bar{K}^*$ degrees of freedom. Our approach, instead provides directly the coupling of the Λ^* to $\bar{K}^*N$ because $\bar{K}^*N$, together with other vector-meson baryon states, are part of the basis of the coupled channels. These latter states are not considered in the coupled channel approach of Ref. [21]. Nevertheless, it is reassuring that the value quoted in [21] for $g'_{K^*N\Lambda^*} \sim 1.5/\sqrt{2} \approx 1.1$ is similar to ours (≈ 0.75), and in anycase it is much smaller than that used in the previous phenomenological studies of the $\gamma p \to K^+\Lambda^*$ reaction.

From the findings of this subsection, we conclude that the K^* mechanism is much smaller than the K one. We drop hereafter completely the K^* contribution in the effective Lagrangian approach.

4.2 $\gamma p \to K^+\Lambda^*$ cross section

We use a hybrid approach, and assume that the quark-gluon string mechanism dominates the $\gamma p \to K^+\Lambda^*$ reaction at photon energies well above threshold, where the experimental data exist. The quark-gluon string model accounts, in principle, for both the K and the K^* Reggeon exchange processes. For these trajectories, we use

$$\alpha_K(t) = -0.20 + 0.8\, t/\mathrm{GeV}^2 \tag{55}$$

$$\alpha_{K^*}(t) = 0.36 + 0.8\, t/\mathrm{GeV}^2, \tag{56}$$

where we have taken slopes around 0.8 [GeV^{-2}] that provide, as we will show, a reasonable description of the $d\sigma/dt$ data, and are not far from the value of around 0.9 used in

[11] The $\sqrt{2}$ factor is implemented here because the value 1.5 quoted in Ref. [21] refers to the $K^*N\Lambda^*$ coupling in isospin basis ($I = 0$).

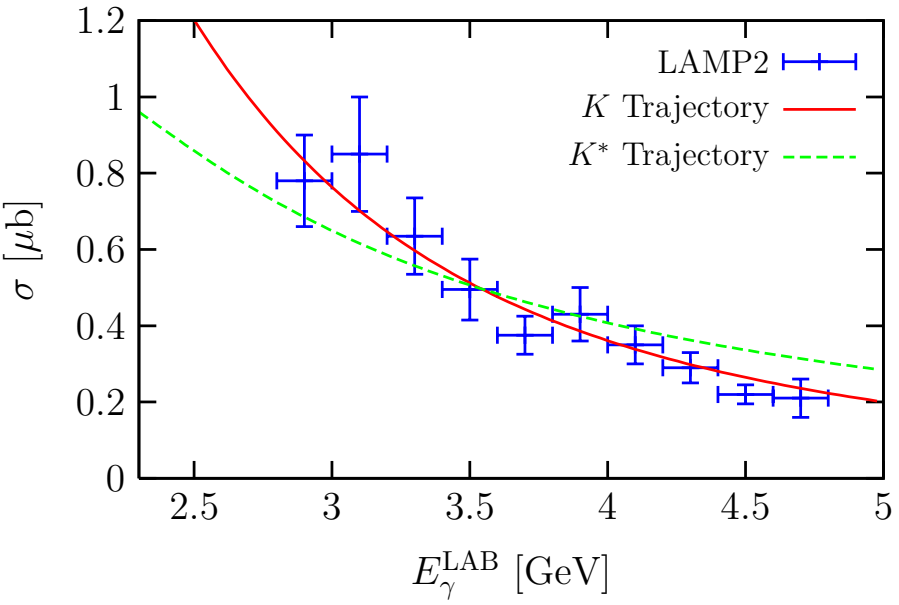

Figure 3: $\gamma p \to K^+\Lambda^*$ total cross section (in units of μb) from the quark-gluon reaction mechanism, as a function of the photon energy in the LAB frame. The solid (dashed) curve has been obtained with the $K-(K^*-)$Regge trajectory. The cutoff parameter a in the gaussian form-factor of Eq. (20) is set to 1 GeV. The experimental data are taken from Ref. [22].

Ref. [14][12] or of 0.93 deduced from the $\rho-$trajectory [32]. The intercepts, $\alpha(0)$, are determined by requiring $\alpha_K(m_K^2) = 0$ and $\alpha_{K^*}(m_{K^*}^2) = 1$.

We show in Fig. 3 the energy dependence of the photon induced Λ^* production cross section with both Regge trajectories. We use a cutoff a in Eq. (20) of 1 GeV, which is of a natural size in hadron physics. To describe the overall normalization of the data, we take $\bar{g}_{\gamma KK}\bar{g}_{KN\Lambda^*} = e g_{KN\Lambda^*} \times 0.12$ and $\bar{g}_{\gamma KK^*}\bar{g}_{K^*N\Lambda^*} = e g_{\gamma KK^*} g_{K^*N\Lambda^*} \times 4.24$. We see that the K Regge trajectory provides a better description of the data than the K^* one in the energy range studied here. Of course, this conclusion is affected by the choice of the cutoff parameter a in the gaussian form-factor of Eq. (20). The larger a, the better description of data is obtained with the K^*-trajectory, since the slope (in absolute value) of the cross section with respect $E_\gamma^{\rm LAB}$ increases. Nevertheless, the description obtained from the $K-$trajectory is always better. To find a more or less comparable description from both trajectories we need to use values of a above 10 GeV. For those values of a and the energies explored in this work, the form-factor F is in practice 1, which is somehow unrealistic. We remind here also that to make both the $K-$ and K^*-Regge contributions similar in size, we should re-scale one over the other by a factor of the order 1200 [$(4.24/0.12)^2$].

Thus, here again we conclude that the K Reggeon mechanism is more favored by data than the K^* Reggeon one, which will be neglected in what follows.

Next, we pay attention to $d\sigma/dt$ and test the dependence of the Regge results on the cutoff parameter a. This differential cross section, averaged over the incident LAB photon energy range 2.8 GeV $\leq E_\gamma^{\rm LAB} \leq$ 4.8 GeV, has been measured in the Daresbury experiment [22]. In Fig. 4, we compare these measurements with our $K-$Reggeon exchange

[12]Note, however, that the K^*-trajectory used in this reference does not lead to $\alpha_{K^*}(m_{K^*}^2) = 1$. Indeed, it is much closer to our $K-$trajectory than to the K^*-one, in the $t-$range $[-1:0]$ GeV^2 of interest in this work.

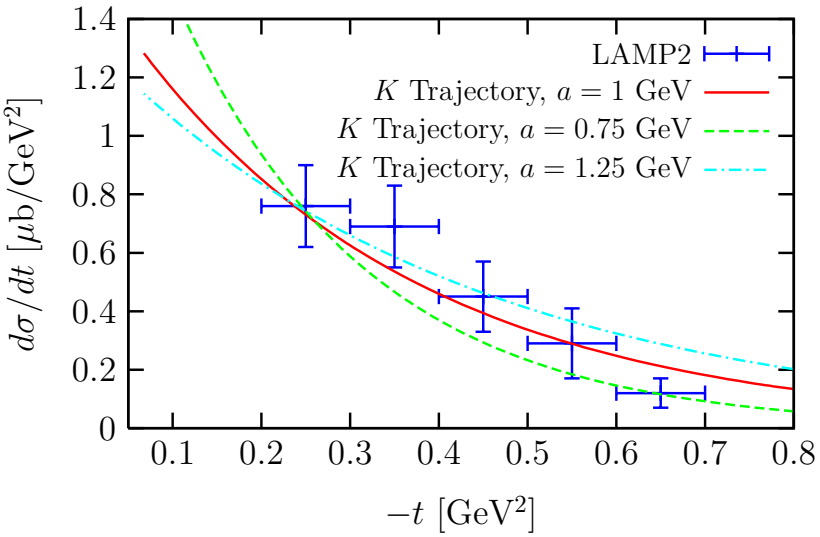

Figure 4: $\gamma p \to K^+\Lambda^*$ differential cross section ($d\sigma/dt$) from the $K-$Reggeon exchange mechanism, as a function of $(-t)$ for $E_\gamma^{\rm LAB} = 3.8$ GeV. We use three values for the cutoff parameter a in the gaussian form-factor of Eq. (20): $a = 1$ GeV, $a = 0.75$ GeV and $a = 1.25$ GeV, which results correspond to the solid, dashed and dash-dotted curves, respectively. In the latter two cases, the results have been scaled up and down by factors 3/2 and 0.85, respectively. The experimental data-points, taken from [22], stand for the $K^+\Lambda^*$ photo-production differential cross section $d\sigma/dt$ averaged over the incident LAB photon energy range 2.8 GeV $\leq E_\gamma^{\rm LAB} \leq$ 4.8 GeV of the Daresbury experiment.

results for three values of a around 1 GeV and using an average energy $E_\gamma^{\rm LAB} = 3.8$ GeV. First, the figure shows that our election for the Regge slope $\alpha'_K(0) \approx 0.8$ [GeV^{-2}] provides a fair description of the $t-$dependence of the differential cross section when the gaussian cutoff is fixed to values around 1 GeV. Second, we see a mild dependence of the results on a, and find that the use of $a = 1$ GeV provides a slightly better description of the $t-$dependence of the differential cross section.

Hybrid hadron/$K-$Reggeon exchange model results for the $\gamma p \to K^+\Lambda^*$ total cross section are shown in Fig. 5 from threshold up to photon energies (in the LAB frame) around 5 GeV. We always neglect the K^*-contributions, both in the hadron and in the quark-gluon string model. In the effective hadron Lagrangian model, we neglect the terms affected by the f_s form-factor, since they are greatly suppressed by it [13]. We have examined two different values of the cutoff Λ entering in the hadron form-factors of Eq. (18), and as can be appreciated in the figure, the predictions depend drastically on the precise used value. For the weighting function of Eq (28), which characterizes the hybrid model, the values $E_0 = 2.3\,$GeV (for $\Lambda = 0.75$ GeV) and $2.0\,$GeV (for $\Lambda = 1$ GeV) and $\Delta E = 0.1\,$GeV have been used.

We also show, in Fig. 5, results from the the K Reggeon exchange model in the entire photon energy range. This latter reaction mechanism leads to cross sections of about 2μb at $E_\gamma^{\rm LAB}$ =2 GeV. It would be highly desirable to count with experimental measurements of the cross section around these energies, for which occur the transition between the hadron and the string quark-gluon reaction mechanisms [11].

Finally, in Fig. 6 we present results for the $E_\gamma^{\rm LAB}$ =2 GeV cm angular distributions from the three models studied in Fig. 5. For all cases the differential cross section peaks forward and gradually fall down as the cm angle increases.

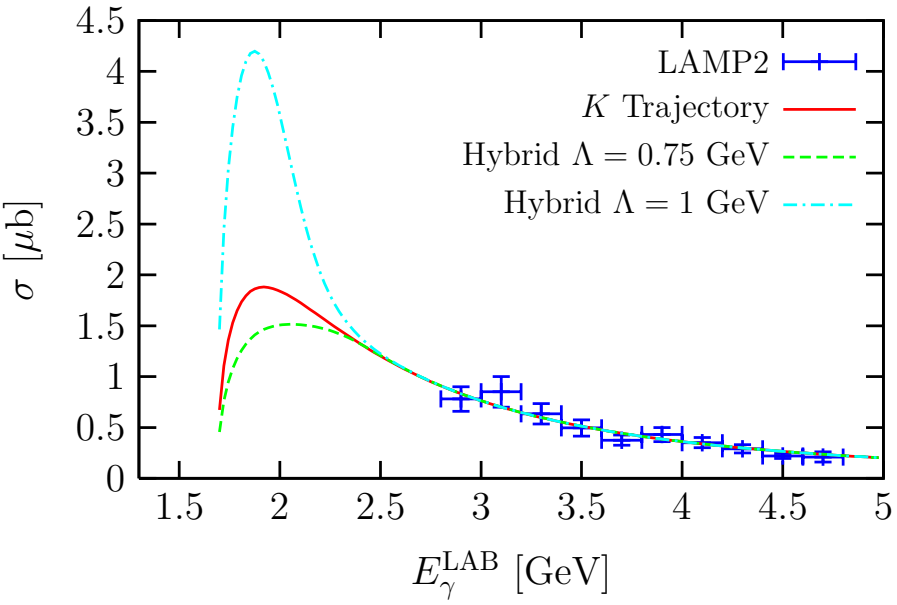

Figure 5: Predictions from different models and data [22] for the $\gamma p \to K^+\Lambda^*$ total cross section as a function of the LAB photon energy. Results from the quark-gluon mechanism ($a = 1$ GeV) are shown by the solid curve. The other two curves display the hybrid hadron/$K-$Reggeon exchange model results (see Subsect. 2.3) for two different values of the cutoff Λ entering in the hadron form-factors of Eq. (18). The dashed and dash-dotted lines stand for the results obtained with $\Lambda = 0.75$ GeV and $\Lambda = 1$ GeV, respectively. In the latter (former) case we use $E_0 = 2.0(2.3)$ GeV, while the parameter ΔE is set in both cases to 0.1 GeV.

5 Conclusion

We have studied the photon induced Λ^* production using both an effective hadron model and a quark-gluon string approach, in a wide range of laboratory photon energies from threshold up to 5 GeV.

We have studied first the coupling constant $g_{K^*N\Lambda^*}$ within the SU(6) chiral unitary model proposed in Ref. [1], and found that this coupling constant is of the order of 0.5. This value is much smaller than both the value used by phenomenological studies and that of $g_{KN\Lambda^*}$, determined by the Λ^* decay width. Hence, we conclude that the contribution of $t-$channel K^* exchange in the effective Lagrangian approach can be safely neglected. We have also discussed the existing connection between the small value found for $g_{K^*N\Lambda^*}$ and the proximity of the Λ^* mass to the $\pi\Sigma^*$ threshold.

We have also shown that the quark-gluon string reaction mechanism, realized in the Reggeon exchange model, is able to reproduce the available experimental data in the region from $E_\gamma^{\rm LAB} \sim 2.8$ GeV up to 5 GeV. Here again, we find that the $K-$trajectory, with a 1 GeV cutoff parameter for the gaussian form-factor, reasonably describes the energy and angular dependence of the cross section.

We should also mention that Titov advocated for the very first time a quark-gluon string approach to study the $\gamma p \to K^+\Lambda^*$ reaction [14]. However, he assumed a clear dominance of the K^* $t-$exchange contribution in the hadron approach near threshold and to describe the higher energy region, where the data lie, he used a reggezation of the K^* meson propagator. We would like to make here two remarks. First, our results for the $K^*N\Lambda^*$ coupling contradict Titov's assumption that the K^* $t-$exchange is the dominant

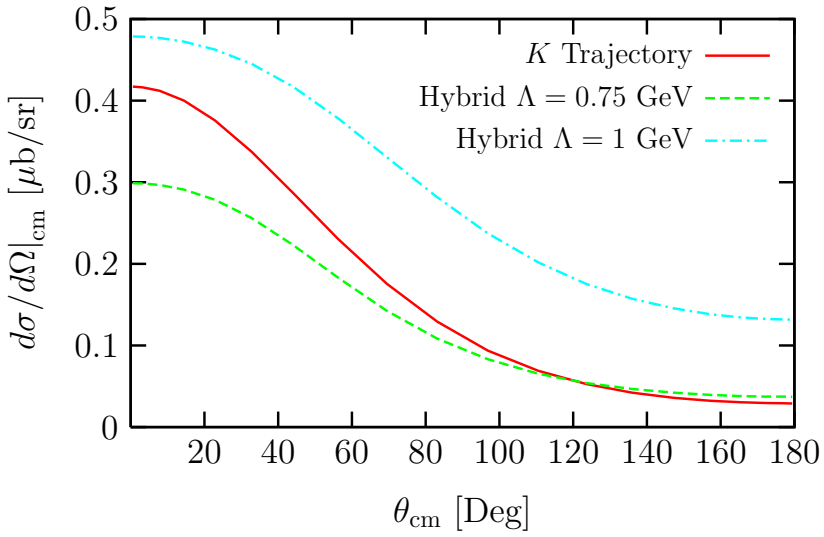

Figure 6: Center of mass differential cross section predicted by the three theoretical models of Fig. 5 for $E_\gamma^{\rm LAB} = 2$ GeV.

mechanism near threshold (he used a value for this coupling around a factor 10 larger than that deduced here). Second, and as we have already mentioned, the K^*-trajectory used in this reference does not lead to $\alpha_{K^*}(m^2_{K^*}) = 1$. Indeed, it is much closer to our $K-$trajectory than to the K^*-one in the $t-$range where the data have been measured.

We have smoothly extended this Reggeon exchange model down to smaller energies and found that it leads to cross sections of around 2 μb in the $E_\gamma^{\rm LAB} \sim 2$ GeV region. We have then proposed a hybrid model to connect with the meson-baryon approach. Finally, we have shown that the effective Lagrangian model predictions depend largely on the hadron form-factor. It would be very important to compare with experimental measurements of the cross sections in the energy region of $E_\gamma^{\rm LAB} \sim 2$ GeV in order to determine this form-factor and also to better understand the transition between the meson-baryon and the quark-gluon mechanisms.

H.T. acknowledges the hospitality of the Departamento de Física Atómica, Molecular y Nuclear, Universidad de Granada, MEC support for *Estancias de Profesores e investigadores extranjeros en régimen de año sabático en España* SAB2006–0150 and the support by the Grant-in-aid for Scientific Research (C)18540269 of the Ministry of Education in Japan. CGR and JN acknowledges support from Junta de Andalucia grant FQM0225, MEC grant FIS2005–00810 and from the EU Human Resources and Mobility Activity, FLAVIAnet, contract number MRTN–CT–2006–035482.

References

[1] C. Garcia-Recio, J. Nieves and L.L. Salcedo, Phys. Rev. **D74** (2006) 034025.

[2] T. Nakano et al., (LEPS Collaboration), Phys. Rev. Lett. **91** (2003) 012002.

[3] S. Stepanyan et al., (CLAS Collaboration), Phys. Rev. Lett. **91** (2003) 252001.

[4] A. Airapetian et al. (HERMES Collaboration), Phys. Lett. **B585** (2004) 213.

[5] N. Kaiser, P.B. Siegel and W. Weise, Nucl. Phys. **A594** (1995) 325; *ibidem* Phys. Lett. **B362** (1995) 23.

[6] E. Oset and A. Ramos, Nucl. Phys. **A635** (1998) 99; D. Jido, J.A. Oller, E. Oset, A. Ramos and U.G. Meissner, Nucl. Phys. **A725** (2003) 181; S. Sarkar, E. Oset and M.J. Vicente–Vacas, Nucl. Phys. **A750** (2005) 294, Erratum-ibid. **A780** (2006) 78.

[7] J. Oller and U. Meissner, Phys. Lett. **B500** (2001) 263.

[8] M. F. M. Lutz and E. E. Kolomeitsev, Nucl. Phys. **A700** (2002) 193; E.E. Kolomeitsev and M.F.M. Lutz, Phys. Lett. **B585** (2004) 243.

[9] J. Nieves and E. Ruiz-Arriola, Phys. Rev. **D64** (2001) 116008; C. García-Recio, J. Nieves, E. Ruiz-Arriola and M. J. Vicente-Vacas, Phys. Rev. **D67** (2003) 076009.

[10] C. García-Recio, M.F.M Lutz and J. Nieves, Phys. Lett. **B582** (2004) 49.

[11] T. Nakano, talk given in 'INPC 2007, International Nuclear Physics Conference', Tokyo, Japan, june 2007 and private communications.

[12] L. Roca, S. Sarkar, V.K. Magas and E. Oset, Phys. Rev. **C73** (2006) 045208.

[13] S.I. Nam, A. Hosaka and H.C. Kim, Phys. Rev. **D71** (2005) 114012.

[14] A.I. Titov, B. Kämpfer, S. Date and Y. Ohashi, Phys. Rev. **C72** (2005) 035206.

[15] A.B. Kaidalov, Z. Phys. **C12** (1982) 63.

[16] A. Donnachie and P.V. Landshoff, Phys. Lett. **B185** (1987) 403.

[17] V. Yu. Grishina, L. A. Kondratyuk, W. Cassing, M. Mirazita and P. Rossi, Eur.Phys.J. **A25** (2005) 141.

[18] C. García-Recio, J. Nieves and L.L. Salcedo, Eur. Phys. J. **A31** (2007) 499.

[19] C. García-Recio, J. Nieves and L.L. Salcedo, Eur. Phys. J. **A31** (2007) 540.

[20] F. Gürsey and L.A. Radicati, Phys. Rev. Lett. **13** (1964) 173; A. Pais, Phys. Rev. Lett. **13** (1964) 175; B. Sakita, Phys. Rev. **136** (1964) B1756.

[21] T. Hyodo, S. Sarkar, A. Hosaka, and E. Oset, Phys. Rev. **C73** (2006) 035209; Erratum-ibid. **C75** (2007) 029901.

[22] D.P. Barber et al., Z. Physik, **C7** (1980) 17.

[23] W.-M.Yao et al. (Particle Data Group), J. Phys. **G33** (2006) 1.

[24] K. Ohta, Phys. Rev. **C40** (1989) 1335.

[25] H. Haberzettl, C. Bennhold, T. Mart, T. Feuster, Phys. Rev. **C58** (1998) R40.

[26] A.B. Kaidalov, L.A. Kondratyuk and D.V. Tchekin, Phys. Atom. Nucl. **63** (2000) 1395.

[27] K. Kubo, Y. Yamamoto and H. Toki, Prog. Theor. Phys. **101** (1999) 615.

[28] C. García-Recio, J. Nieves and L.L. Salcedo, Phys. Rev. **D74** (2006) 036004.

[29] C. García-Recio, J. Nieves and L.L. Salcedo, Eur. Phys. J. **A31** (2007) 491.

[30] J.J. de Swart, Rev. Mod. Phys. **35** (1963) 916.

[31] J.C. Carter, J.J. Coyne and S. Meshkov, Phys. Rev. Lett. **14** (1965) 523; *erratum* Phys. Rev. Lett. **14** (1965) 850.

[32] A. Donnachie and P.V. Landshoff, Phys. Lett. **B296** (1992) 227.